

Synthesis of ZnO-TiO₂ Nanoparticles by Sol-Gel Process and its Application for Solar Cell Semiconductor

Nanda Saridewi^{1*}, Aditya Riyanti², Isalmi Aziz², Ade Lian Risa Adinda², Biaunik Niski Kumila³

¹Department of Chemistry Education, Faculty of Tarbiya and Teaching Science UIN Syarif Hidayatullah Jakarta, Jl. Ir. H. Juanda No. 95 Ciputat, Tangerang Selatan 15412, Indonesia.

²Department of Chemistry, Faculty of Science and Technology, UIN Syarif Hidayatullah Jakarta, Jl. Ir. H. Juanda No. 95 Ciputat, Tangerang Selatan 15412, Indonesia.

³Department of Physics, Faculty of Science and Technology, UIN Syarif Hidayatullah Jakarta, Jl. Ir. H. Juanda No. 95 Ciputat, Tangerang Selatan 15412, Indonesia.

Email: nanda.saridewi@uinjkt.ac.id

Article Info

Received: May 10, 2023
Revised: September 14, 2023
Accepted: October 15, 2023
Online: November 30, 2023

Citation:

Saridewi, N., Riyanti, A., Aziz, I., Adinda, A. L. R., & Kumila, B. N. (2023). Synthesis of ZnO-TiO₂ Nanoparticles by Sol-Gel Process and its Application Thereof as Solar Cell Semiconductor. *Jurnal Kimia Valensi*, 9(2), 261-270.

Doi:

[10.15408/jkv.v9i2.32206](https://doi.org/10.15408/jkv.v9i2.32206)

Abstract

ZnO-TiO₂ semiconductors can be used in Dye-Sensitized Solar Cell (DSSC) devices as an alternative to renewable energy. This semiconductor can be synthesized by the sol-gel method. The objective of this study is to synthesize the TiO₂-doped ZnO nanoparticle semiconductors for DSSC devices with mangosteen peel extract dye. Avocado seeds were extracted with water, as a capping agent in the synthesis of ZnO-TiO₂ (TiO₂ ratio of 0,3,5,7 and 10% to ZnO). XRD results show the success of ZnO-TiO₂ doping, due to the 2θ shift and changes in the crystal lattice. The average crystal size obtained was 33.7972 nm. The SEM results showed that the particle size of ZnO ranged from 45-100 nm. The UV-Vis dye measurements of mangosteen peel extract showed an absorption peak at 296-483 nm wavelength, with a corresponding band gap energy value of 3.04 eV. The UV-Vis DRS ZnO-TiO₂ measurements have an average band gap energy of 3.1425 eV and ZnO of 3.1915 eV. The highest DSSC efficiency value is 2.15 x 10⁻²% at 7% ZnO-TiO₂ semiconductor.

Keywords: Doping, TiO₂-ZnO nanoparticles, dye-sensitized solar cell (DSSC)

1. INTRODUCTION

The TiO₂ semiconductors are materials that have strong oxidizing power, good stability against corrosion, and a nanopore structure that can absorb large amounts of dye molecules. TiO₂ has gap energy between 3.2-3.8 eV. Another semiconductor that has similar gap energy with TiO₂ is ZnO which has a wider band energy gap (≥3.37 eV) thus promising as materials to be used in solar cell device¹. The disadvantage of ZnO is that they have lower stability than TiO₂. However, ZnO has higher electron mobility and higher exciton binding energy (60 meV) which allows exciton emission at room temperature². The cost of ZnO production is more efficient i.e., up to 75% compared to that of TiO₂. Therefore, it is recommended to be used as raw material for heterogeneous photocatalysts.

Semiconductors with lower band gap energy can be applied to photovoltaic cells such as dye-sensitized solar cells (DSSC). The Dye Sensitized Solar Cell is a solar cell generation with great potential for the future since DSSC does not require highly purified material thereby lowering the production cost. The DSSC device is able to convert solar energy as renewable energy into electrical energy³. In said DSSC device, light absorption, and electric charge separation processes occur separately^{4,5}. The dye molecule acts as a light absorber whilst charge separation is accelerated by organic semiconductor molecules with wider gap energy⁶, widening the absorption spectrum and increasing the number of electrons flowing from the conduction band to the valence band⁷. Mangosteen peel (*Garcinia mangostana*) is one of agricultural waste that can be used as dye molecules. The main component in the mangosteen

peel extract is α -mangostin and anthocyanin which can be applied in the DSSC device^{8,9}.

The synthesis of ZnO-TiO₂ can be carried out by sol-gel method. The sol-gel method is utilized to synthesize oxidizing materials since this method allows a very simple control in terms of particle sizes and experimental processes. The main advantage of this method is the homogeneity of the highly pure sol-gel product, good physical-chemistry characteristics, and good surface morphology¹⁰. This bottom-up approach with the green synthesis method can be used as an alternative in synthesizing more environmentally friendly nanoparticles with plant extract (leaf, root, flower, fruit, seed, and the like) as raw material¹¹.

The avocado seed extract can be used in the synthesis process of the nanoparticles as a capping agent. The Avocado (*Persea americana*) seed is rich in bioactive components such as phenolics, flavonoids, tannin, ascorbic acid, tocopheryl acetate, and carotenoids thereby it has plenty of functional groups which can act as capping agents in nanoparticle synthesis¹². The objective of this research is to synthesize ZnO-TiO₂ nanoparticles using the extract of Avocado seed as a capping agent and its application thereof as a semiconductor in DSSC.

2. RESEARCH METHOD

Tools

Schott duran erlenmeyer flask 500 mL, schott duran beaker glass 600 mL, analytical balanced, pH indicator, porcelain cup 25 mL and 50 mL, filter paper, funnel, mortar, pestle, magnetic stirrer, hotplate, thermometer, furnace, centrifuge, oven and grinder, x-ray diffraction (Bruker D2 Phaser), UV-Vis Diffuse Reflectance Spectroscopy (Shimadzu UV-2450), scanning electron microscope (Hitachi S-3400N)

Materials

Materials used in this research is Avocado seed extract, Zinc acetate dihydrate (Zn(CH₃COO)₂·2H₂O) (Merck), Titanium (IV) oxide (Ti(OCH₂CH₃)₄) (Merck), NaOH (Merck), methanol, and polyethylene glycol gel electrolyte(PEG), KI/I₂.

Procedure

Avocado Seed Extract

Dried Avocado (*Persea americana*) seeds were mashed, subsequently weighed 10 grams and placed in a beaker, then 100 mL of distilled water was added, and a magnetic stirrer was placed in the beaker. The extract was heated in a water bath at 100 °C for 25 minutes. Heating is carried out while

constantly stirring under a stirring speed of 400 rpm¹³. The extract was filtered using filter paper Whatman No. 41. The resulting avocado seed extract was used for the synthesis of ZnO-TiO₂ nanoparticles.

Synthesis of ZnO-TiO₂ Nanoparticles

The first step of synthesizing TiO₂ doped ZnO includes the preparation of the mixture of acetate-Zn and Ti-ethoxy solutions at a concentration of 0.15 M and concentration variation of TiO₂ 3% (0.0359 g) 97% ZnO (3.1936 g), 5% TiO₂ (0.0599 g) 95% ZnO (3.1277 g), 7% TiO₂ (0.0839 g) (3.0619 g) and 10% TiO₂ (0,1198 g) 90% ZnO (2,9631 g) in 100 mL by volume of mixture solution. Extract filtrate of the avocado seed was taken on 10 ml and was added with 90 mL of ZnO-TiO₂ 0.15 M, subsequently the solution was heated at 70°C for 1 hour on a water bath constantly stirred for 1 hour to obtain sol ZnO-TiO₂. The precipitate was collected by centrifuge at 25°C at 4000 rpm for 10 mins. The precipitate was rinsed with distilled water and dried in an oven at 100°C for 18 hours. The precipitate further calcinated at 450°C for 4 hours in a furnace¹⁴.

Preparation of Dye from Mangosteen Peels

The extract of dried and ground mangosteen peels was weighed at 20 g with analytical balance and added with methanol 100 mL. Subsequently heated in a water bath at 60 °C for 30 mins under constant stirring of 400 rpm. After completion, the extract was filtered, and the maximum wavelength was measured with the mode scanning method.

Efficiency Test on Semiconductor Material TiO₂-ZnO with DSSC

Test using the DSSC was conducted by assembling the testing device. The ITO glass was cleaned using ethanol and dried at 100°C for 15 mins. The ITO glass 4x3 cm² was glued together with adhesive until 2.5 x 2 cm² remained in the middle of the substrate. The substrate was evenly layered with pasted ZnO-TiO₂ by mixing (0.5 g ZnO-TiO₂ with 1 ml glacial acetic acid and 0.1 mL Triton X-100) It was further dried on a hotplate at 30-40°C for an hour. The paste of ZnO-TiO₂ was immersed in the mangosteen peel dye solution for one night. The ZnO-TiO₂ layer was covered with a carbon resistance electrode (electrode-n) and clamped at its both sides in a sandwich structure. Coating the polyethylene glycol (PEG) gel electrolyte between both electrodes layered with PEG polymer gel. Testing the performance efficiency of DSSC through current measurement.

The DSSC measurement series was performed using potentiometers, multimeters, and sunlight as the light source with an intensity of 760 Lux (0.1113 watt/cm²)¹⁵.

The DSSC efficiency was calculated using the following formula:

$$\eta = \frac{P_{max}}{P_{light}} \times 100\% \quad (1)$$

3. RESULT AND DISCUSSION

Characterizing the ZnO-TiO₂ nanoparticles using the XRD

Based on the XRD measurement, the diffraction peak was found located at angle 2θ of 25.2° - 25.3° as the TiO₂ peak in the sample of ZnO-TiO₂ nanoparticles sample (3.57 and 10%) where the standard peak of TiO₂ has the highest peak value at 2θ angle (26.686°). The intensity of the diffraction peak is increasing with the increasing ratio of TiO₂ concentration as a result of increasing the angle 2θ value in the nanoparticles which

indicates that more TiO₂ is not doped and dispersed in the nanoparticles.

The doping of TiO₂ toward the ZnO particles may cause a shift in the value of 2θ. The shift of 2θ angles occurring in the sample is the parameter of success in the doping process of ZnO-TiO₂. The TiO₂ doping results in peak shifting at 2θ position (°) 31, 36, 47, 56, and 67 shift toward higher 2θ(°) and peak broadening. This indicates lattice changes and crystalline defects as a result of the TiO₂ dopants (Ti⁴⁺) substituted at the ZnO crystal lattice. The difference in the ion Zn²⁺ radius (0,74 Å) and Ti⁴⁺ (0,605 Å) may result in distortion on the ZnO structure, lattice strain, and crystal defect¹⁶. The presence of TiO₂ dopants in the ZnO results in the formation of a new compound in the ZnO doping sample 10% TiO₂ namely the compounds Zn₂TiO₄ and ZnTiO₃ marked by peaks in the area of 34,5°- 36° with JCPDS standard Zn₂TiO₄ No. 73.0578 and JCPDS ZnTiO₃ No. 85-0547¹⁷.

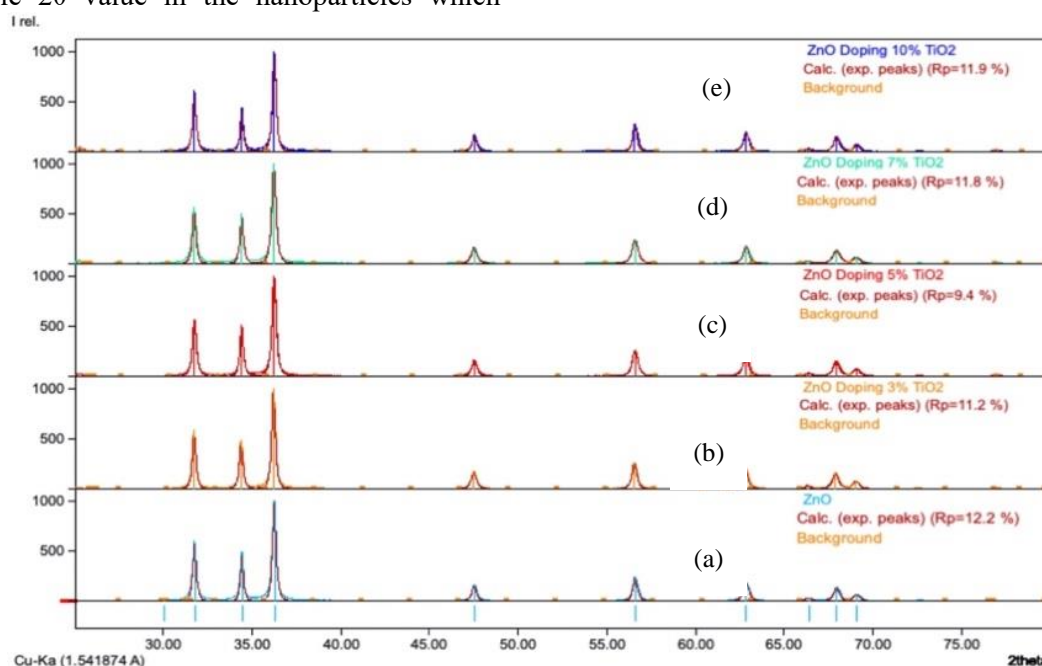


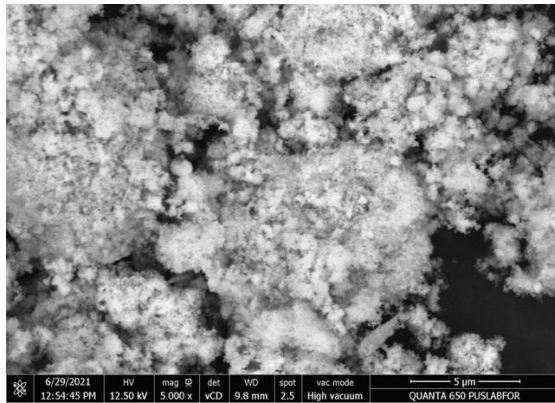
Figure 1. Nanoparticles Diffraction Pattern at 0,15 M pH 8 (a) ZnO; (b) ZnO-TiO₂ 3%; (c) ZnO-TiO₂ 5%; (d) ZnO-TiO₂ 7%; (e) ZnO-TiO₂ 10%.

Table 1. Crystal lattice parameters

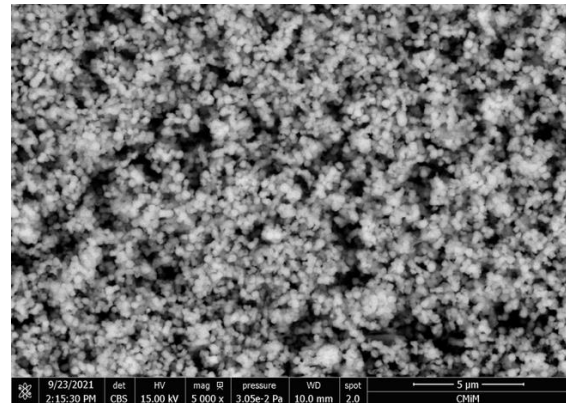
No	Sample	Lattice parameter values		
		a (Å)	b (Å)	c (Å)
1	ZnO	4.9521	4.3631	5.6226
2	ZnO-TiO ₂ 3%	5.2017	5.6661	4.6843
3	ZnO-TiO ₂ 5%	5.2023	5.6308	4.6559
4	ZnO-TiO ₂ 7%	5.2017	5.6338	4.6531
5	ZnO-TiO ₂ 10%	5.1370	5.4895	4.6148

Table 2. Crystal Size and Profile Residue of ZnO-TiO₂

No	Sample	FWHM (°)	Crystal size (nm)	Rp (%)
1	ZnO	0.244	34.2744	12.2
2	ZnO-TiO ₂ 3%	0.249	33.6620	11.2
3	ZnO-TiO ₂ 5%	0.267	33.4354	9.4
4	ZnO-TiO ₂ 7%	0.256	31.3219	11.8
5	ZnO-TiO ₂ 10%	0.231	36.2926	11.9



(a)



(b)

Figure 2. Surface morphology of nanoparticles (a) ZnO and (b) ZnO-TiO₂ 7%

The TiO₂ dopants tend to cause a decrease in crystal lattice parameters in which the decrease occurs in the cell unit of *a*, *b*, and *c* at ZnO-TiO₂ (3, 5, 7, and 10%). The parameter decrease in those cell units was a result of substitution at the Ti⁴⁺ ion and substituting the position of Zn⁺² ions in the ZnO lattice¹⁸. The ion Ti⁴⁺ radius (0,605 Å)¹⁹ is smaller compared to that of ion Zn⁺² radius (0,74 Å)¹⁶ which results in a decrease of the ZnO crystal lattice parameters²⁰. The Ti⁴⁺ substitution also results in a decrease of the crystal size, and the increasing amount of doping will lead to more dislocation on the crystal thereby resulting in a smaller crystal size in the sample²¹.

The Residue Profile (*Rp*) obtained from XRD data processing is one of the crystallinity parameters of a nanoparticle. The 5% Zn-TiO₂ sample has the smallest *Rp* value of 9.4%. Regarding crystal size, 7% ZnO-TiO₂ sample measures 31.3219 nm. The crystal size has a direct relationship with the surface area, where the smaller the crystal size, the larger the surface area that is able to interact thereby increasing the activity of the nanoparticles²². Thus, in view of the particle size and diffraction pattern, the ZnO doped

7% TiO₂ sample gives the best result compared to other samples that have been synthesized.

Morphology SEM of nanoparticles ZnO and ZnO-TiO₂ 7%

Figure 2 The surface morphology of 7% ZnO and ZnO-TiO₂ with the overall distribution of particles seen in spherical morphology in both samples. Figure 2 (a) shows that there is agglomeration between particles in the ZnO sample. ZnO tends to agglomerate quickly, so the nanoparticle size becomes more prominent and unstable²³. Agglomeration of ZnO nanoparticles occurred due to the influence of polarity, ZnO electrostatic power, and enormous energy on the surface of nanoparticles during the synthesis process^{13,24,25}. Besides that, agglomeration is thought to happen because many chemical compounds in avocado seed extract react with other molecules^{14,26}. In addition, agglomeration can be caused by a dispersion process during measurement, and no screening process is carried out first. Figure 3 (b) shows that the ZnO-TiO₂ 7% sample produced a smaller particle surface with a homogeneous distribution.

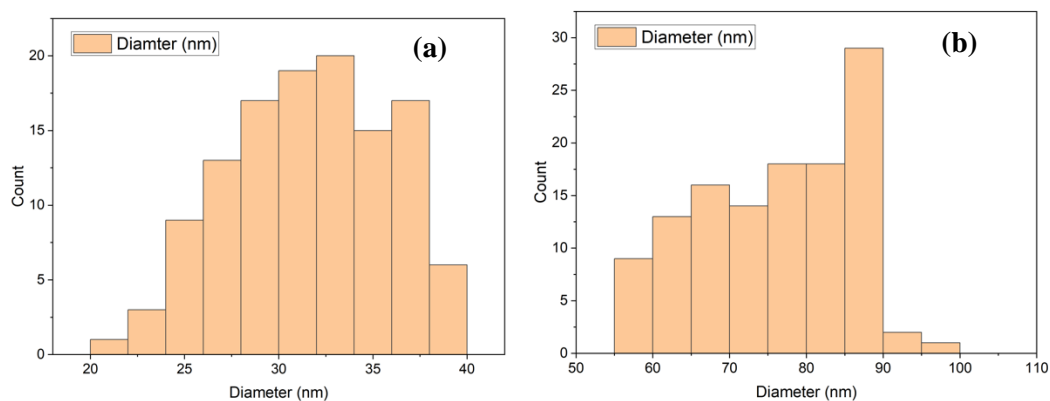


Figure 3. ZnO-TiO₂ particle size distribution (a) ZnO and (b) ZnO-TiO₂ 7%

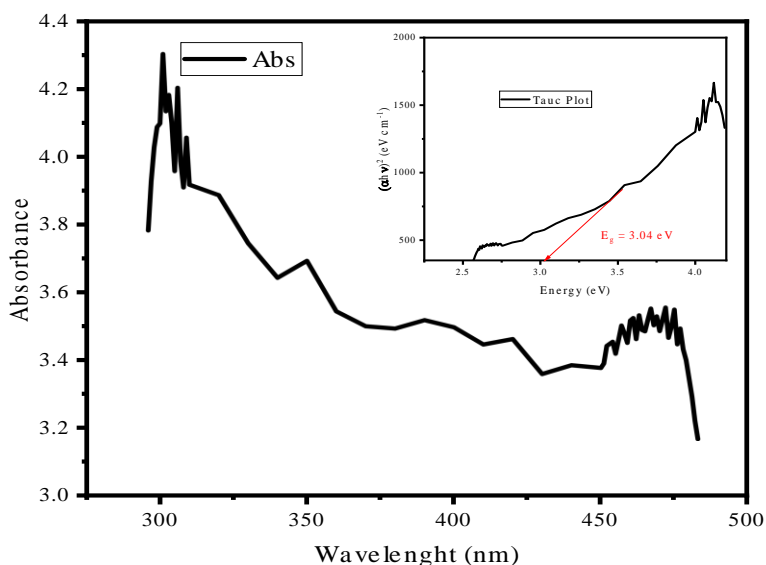


Figure 4. Measurement of Wavelength and Absorbance of Mangosteen Peel Extract

The size distribution of ZnO and ZnO-TiO₂ was measured using SEM and interpreted using ImageJ, by taking 100 diameters nanoparticles of each sample from the SEM image and using Match!3 for interpreted average particle size. Based on interpretations from ImageJ and Match!3 the size distribution of ZnO nanoparticles is between 45-100 nm, with an average particle diameter of 89.53 nm (Figure 3(a)). Meanwhile, the distribution of 7% ZnO-TiO₂ nanoparticles is between 20–40 nm with an average diameter of 31.82 nm (Figure 3(b)). The substitution of Ti⁴⁺ ions can cause a decrease in particle size on the surface, resulting in a larger surface area to be utilized in photocatalyst applications.

Dye Energy Band Gap

The result of the mangosteen peel extract's absorbance measurement was obtained at a wavelength range of 296 to 483 nm with a maximum wavelength of 301 nm. Based on the measurement result of energy band gap of mangosteen peel extract using the Tauc Plot equation, the energy gap value is obtained as 3.04 eV. The obtained band gap value is within the semiconductor range, therefore, indicates that the mangosteen peel extract is sufficient as the dye in the DSSC device as semiconductors. In the DSSC device, the mangosteen peel extract acts as type-p semiconductor. The Energy band gap in the mangosteen peel extract is able to excite the electrons from *Highest Occupied Molecular Orbital* (HOMO) to the state of *Lowest Unoccupied Molecular Orbital* (LUMO), thereby the type-p semiconductors will lose electrons and generate hole²⁷.

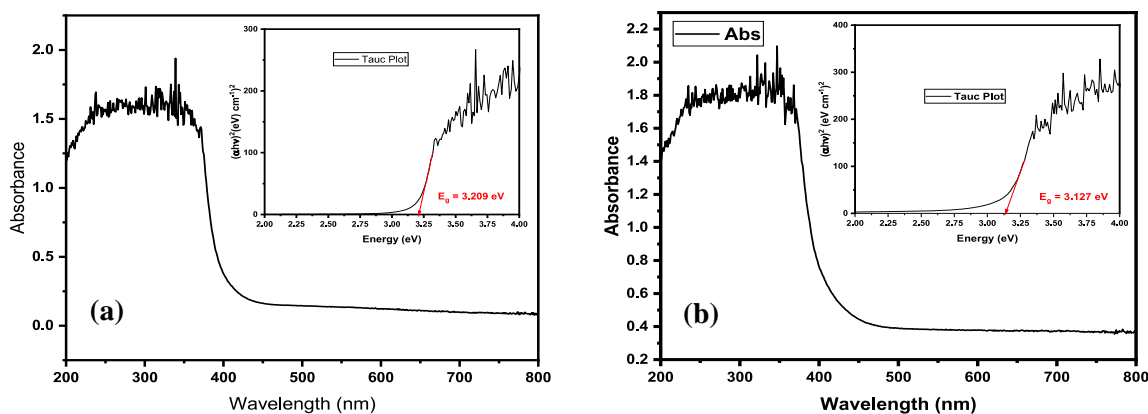


Figure 5. Wavelength Absorbance (a) ZnO; (b) ZnO-TiO₂ 7%

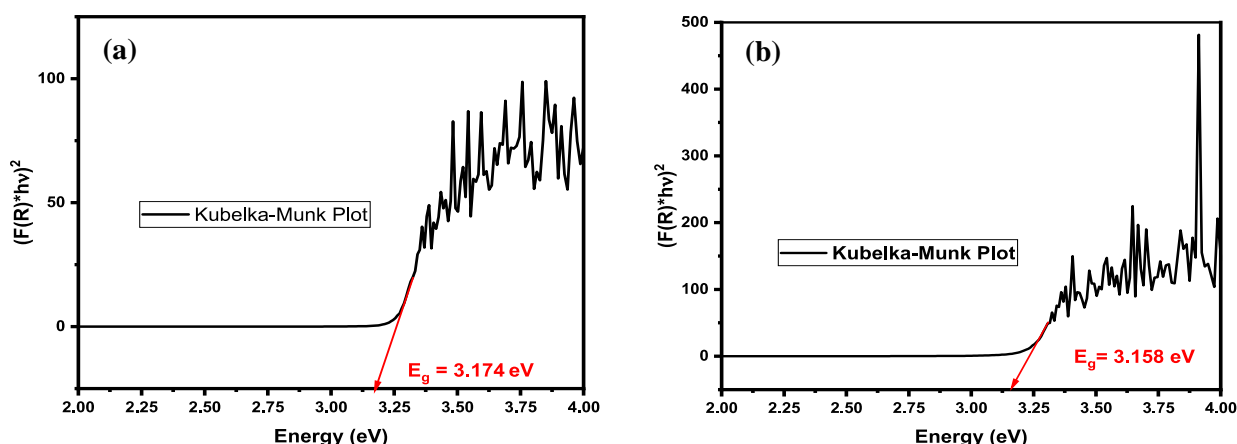


Figure 6. The Graft of Kubelka-Munk Plotting the Band Gap Energy (a) ZnO; (b) ZnO-TiO₂ 7%

Energy Band Gap of ZnO-TiO₂ Semiconductors

Based on Figure 5, 7% ZnO and ZnO-TiO₂ produce wavelength in visible light areas. This is following the study by Dewi et al which reported that ZnO maximum absorbance is obtained at 300-390 nm wavelength²⁸. TiO₂ maximum absorbance is obtained at wavelength 250-450 nm²⁹.

The doping of TiO₂ on samples does not affect the absorbance area since TiO₂ has an absorbance area in visible light, the same as ZnO. Accordingly, both ZnO and TiO₂ experience a decrease in absorbance at a wavelength over 400 nm which is a visible light area, thereby, the light absorbance can be modified with other semiconductors, i.e., dyes from the mangosteen peel extract.

Based on the obtained band gap energy value, the doping of TiO₂ to ZnO resulted in lower band gap energy. This change of band gap energy was caused by the difference in the band gap energy value between ZnO and TiO₂. The valence

band or conduction band in semiconductor material will increase with the addition of dopant, thus change will occur to reflectance or absorbance which in turn leads to the change in band gap energy³⁰. 7% TiO₂ dopant has been shown as capable of reducing the value of band gap energy which in turn will increase its photocatalytic activity in the *dye-sensitized solar cell* (DSSC) device. The 7% ZnO-TiO₂ semiconductors will act as type-n semiconductors in the DSSC device. Dahlan et al have reported that the value of band gap energy for semiconductor-p should be lower than that of band gap energy for type-n semiconductor³¹. Load separation occurs in the DSSC, when the photon energy from visible ray appears to be absorbed, the electrons at the type-p semiconductors (in dyes) will be excited from the HOMO stated (highest occupied molecular orbital) to LUMO state (lowest unoccupied molecular orbital) subsequently, the electrons will be transferred to the conduction band of type-n semiconductors.

Application of ZnO-TiO₂ Semiconductor to DSSC Device

The relationship between I -V curve and resistance in above Figure 7 indicates that as the resistance increases, the resulting voltage also

increases and conversely, as the resistance increases, the Intensity value decreases.

Data collected, such as maximum intensity I_{max} , maximum voltage (V_{max}), maximum power (P_{max}), and fill factor value (FF) are processed using Microsoft Excel to obtain efficiency value (η).

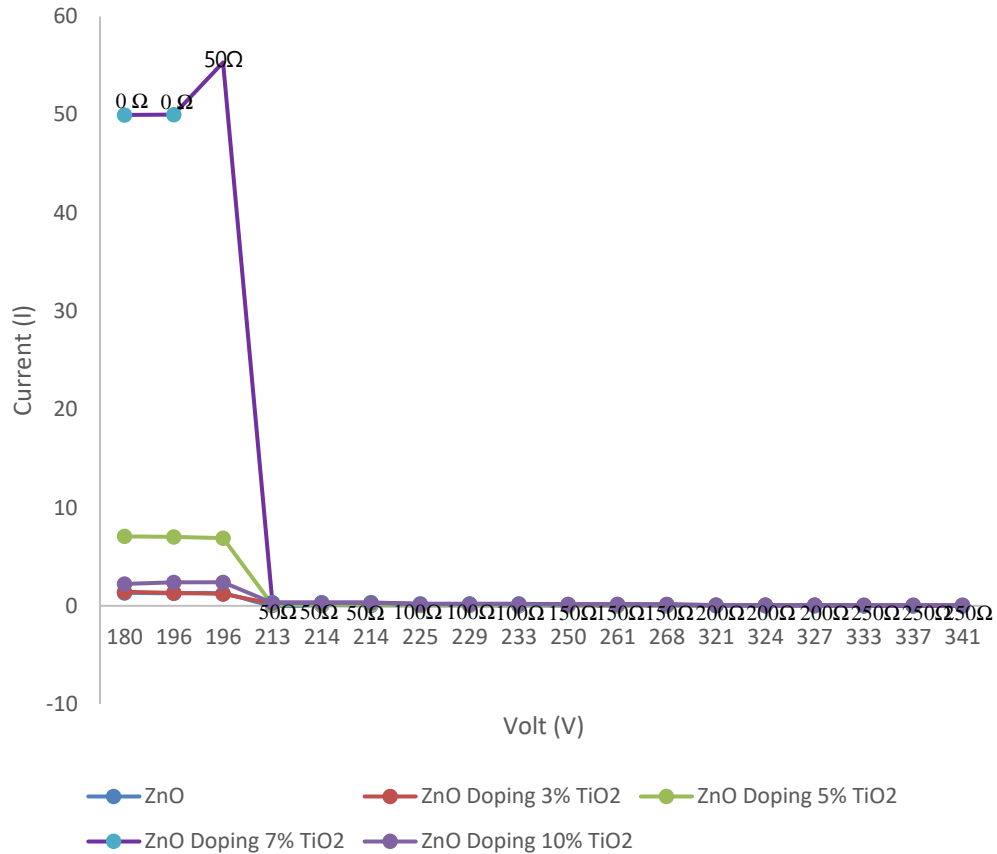


Figure 7. Relation between Intensity and Voltage (I-V)

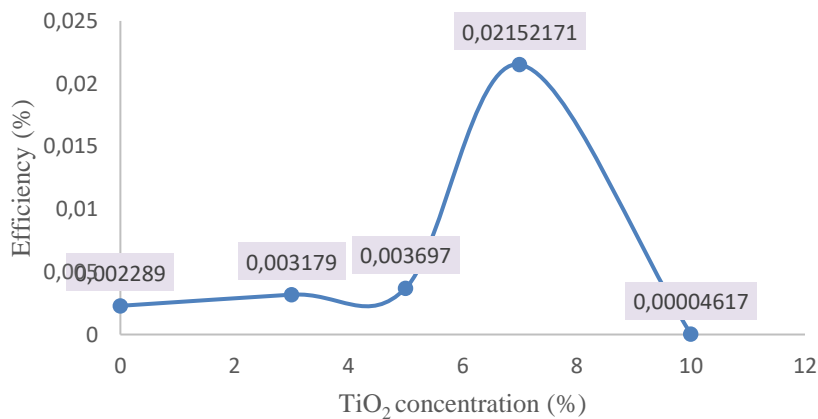


Figure 8. Effect of TiO₂ Concentration to the DSSC Efficiency

Significantly, the addition of TiO₂ dopant is able to increase the DSSC efficiency in all samples, non-doped TiO₂ sample is able to increase the semiconductor activity in DSSC due to having a larger band gap energy value than that of ZnO. In general, ZnO has point of zero (pzc) at pH of 8-9³² whereas TiO₂ has a pzc of pH 5.5-6.5³³. Meanwhile, the value of pH for dyes during the sensitization process will work effectively at pH 5.

ZnO semiconductor based- DSSC would therefore has lower efficiency since at pH under the pzc semiconductor will tend to be acidic. The ZnO surface would tend to have positive charge (Zn²⁺) and be able to pull anions from the dyes to form a new complex. Meanwhile, the TiO₂ has pH which corresponds to the dyes pzc, therefore the semiconductor has neutral property and the complex of metal ion dyes could not occur¹⁹.

Doped TiO₂ in the ZnO of DSSC semiconductors has better ability in improving the DSSC efficiency with the highest efficiency value obtained from DSSC device with ZnO doped 7% TiO₂ semiconductor at 2,1521 x 10⁻² %. In DSSC device with ZnO doped 10% TiO₂ semiconductors, the efficiency value is decreased to 4.617 x 10⁻⁴ %. Moreover, based on the XRD result on sample ZnO doped 10% TiO₂ semiconductors, new compounds of Zn₂TiO₄ and ZnTiO₃ have been formed. The formation of compound Zn₂TiO₄ will caused a photoinactive in the ZnO-TiO₂ sample thus resulted in decreasing photocatalytic activity in the sample^{34,35}.

4. CONCLUSION

Sol-gel method is suitable for the synthesis of ZnO-TiO₂ because it produces a good crystal phase with a small particle size, so it can be used for DSSC as a type-n semiconductor with mangosteen peel as a type-p semiconductor. Characteristic of ZnO-TiO₂ 7% nanoparticles has excellent crystal phase with a crystal size of 31.3219 nm, particle size is between 20–40 nm with an average diameter of 31.82 nm and a band gap energy of 3.1425 eV. The highest DSSC efficiency is generated from the ZnO-TiO₂ 7% sample at 2.15 x 10⁻² %.

ACKNOWLEDGEMENT

The authors extend their gratitude to the Indonesian Ministry of Religion Litapdimas for the 2020 research grant at UIN Syarif Hidayatullah so that the research can be performed properly.

REFERENCES

1. Dhanemozhi C, Rajeswari V, Sathyajothi S. Green Synthesis of Zinc Oxide Nanoparticle Using Green Tea Leaf Extract for Supercapacitor Application. *Materials Today Proceedings*. 2017;4(2):660–667. doi:10.1016/j.matpr.2017.01.070
2. Rahman A. Fabrication and Characterization of ZnO Nanoparticles for Sensitized Dye Solar Cell Applications, Tesis, Universitas Indonesia, 2011.
3. Hagfeldt A, Boschloo G, Sun L, Kloo L, Pettersson H. Dye-Sensitized Solar Cells. *Chem. Rev.*, 2010;110(11):6595–6663. doi:10.1021/cr900356p
4. Grätzel M. Dye Sensitized Solar Cells. *Journal of Photochemistry and Photobiology C Photochemistry Reviews*. 2003;42(2):145–153. doi:10.1016/S1389-5567(03)00026-1
5. Grätzel M, Kay A. Low cost photovoltaic modules based on dye sensitized nanocrystalline titanium dioxide and carbon powder. *Solar Energy Materials and Solar Cells*, 1996;44(1):99–117. doi:10.1016/0927-0248(96)00063-3
6. Smestad GP, Grätzel M. Demonstrating Electron Transfer and Nanotechnology: A Natural Dye-Sensitized Nanocrystalline Energy Converter. *Journal of Chemical Education*, 1998;75(6):752–756. doi:10.1021/ed075p752
7. Prasatya AN, Susanti D. Pengaruh Suhu dan Konsentrasi Kalsinasi pada Kaca FTO yang di-Coating ZnO terhadap Efisiensi DSSC yang Menggunakan Dye dari Buah Terung Belanda. *Jurnal Teknik POMITS* 2013;2(2):378–383. doi:10.12962/j23373539.v2i2.3830
8. Wittenauer J, Falk S, Schweiggert-Weisz U, Carle R. Characterisation and quantification of xanthenes from the aril and pericarp of mangosteens (*Garcinia mangostana* L.) and a mangosteen containing functional beverage by HPLC–DAD–MSn. *Food Chemistry*, 2012;134(1):445–452. doi:10.1016/j.foodchem.2012.02.094
9. Zarena AS, Sankar KU. Xanthenes Enriched Extracts From Mangosteen Pericarp Obtain by Supercritical Carbon Dioxide Process. *Separation and Purification Technology*, 2011;80(1):172–178. doi:10.1016/j.seppur.2011.04.027

10. Bhatti K, Khan M, Saleem M, Alvi F, Raza R, Rehman S. Analysis of multilayer based ZnO and TiO₂ photoanodes for dye- sensitized solar cells. *Materials Research Express*, 2019;6(7):1–13. doi:10.1088/2053-1591/ab11e8
11. Sarkar S, Sarkar S, Bhattacharjee C. Green Synthesis of Novel Photocatalysts. *Nanophotocatalysis and Environmental Applications*, 2019;29:241–261. doi:10.1007/978-3-030-10609-6_9
12. Ge Y, Si X, Cao J, Zhou Z, Wang W, Ma W. Morphological characteristics, nutritional quality, and bioactive constituents in fruits of two avocado (*Persea americana*) varieties from Hainan Province, China. *Journal of Agricultural Science*, 2017;9(2):8. doi:10.5539/jas.v9n2p8
13. Azizi S, Ahmad MB, Namvar F, Mohamad R. Green biosynthesis and characterization of zink oxide nanoparticles using brown marine macroalga *Sargassum muticum* aqueous extract. *Materials Letters*, 2014;116:275–277. doi:10.1016%2Fj.matlet.2013.11.038
14. Sari RN, Saridewi N, Shofwatunnisa S. Biosintesis Dan Karakterisasi Nanopartikel ZnO Dengan Ekstrak Rumput Laut Hijau *Caulerpa* Sp. *Jurnal Perikanan Universitas Gadjah Mada*, 2017;19(1):17–28. doi:10.22146/jfs.24488
15. Maryani D, Gunawan G, Khabibi K. Penentuan Efisiensi DSSC (Dye-Sensitized Solar Cell) yang Dibuat dari Semikonduktor ZnO yang diemban Fe³⁺ Melalui Metode Presipitasi. *Jurnal Kimia Sains Dan Aplikasi*, 2012;15(1):29–35. doi:10.14710/jksa.15.1.29-35
16. Shidpour R, Simchi A, Shidpour R, Ghanbari F. Photodegradation of Organic Dye by Zinc Oxide Nanosystems With Special Defect Structure : Effect of Morphology and Annealing Temperature. *Journal Applied Catalys A: General*, 2014;472(2):198–204. doi:10.1016/j.apcata.2013.12.003
17. Jung JS, Kim YH, Gil SK, Kang DH. Dielectric properties of zinc titanate thin films prepared by Rf magnetron sputtering. *Journal of Electroceramics*, 2009;23:272–276. doi:10.1007/s10832-008-9423-4
18. Zhang S, Cao Q, Yao Y. Synthesis and infrared emissivities of Mn- doped ZnO:Co powders. *Infrared Physics & Technology*, 2013;61:1–4. doi:10.1016/j.infrared.2013.07.004
19. Wang C, Xu BQ, Wang X, Zhao J. Preparation and photocatalytic activity of ZnO/TiO₂/SnO₂ mixture. *Journal of Solid State Chemistry*, 2005;178(11):3500–3506. doi:10.1016%2Fj.jssc.2005.09.005
20. Lu Y, Lin Y, Xie T, Shi S, Fana H, Wang D. Enhancement of visible-light-driven photoresponse of Mn/ZnO system: photogenerated charge transfer properties and photocatalytic activity. *Nanoscale*, 2012;4:6393–6400. doi:10.1039/C2NR31671D
21. Naik EI, Naik HSB, Viswanath R, Kirthan BR, Prabhakara MC. Effect of zirconium doping on the structural, optical, electrochemical and antibacterial properties of ZnO nanoparticles prepared by sol-gel method. *Chemical Data Collections*, 2020;29: 100505. doi:10.1016/j.cdc.2020.100505
22. Kohls JJ, Beaucage. Rational Desing of Reinforced Rubber. *Current Opinion in Solid State and Materials Science*, 2002;6(3):183–194. doi:10.1016/S1359-0286(02)00073-6
23. Yunita Y, Nurlina N, Syahbanu I.. Sintesis Nanopartikel Zink Oksida (ZnO) dengan Penambahan Ekstrak Klorofil sebagai Capping Agent. *Positron*, 2020;10(2):44. doi:10.26418/positron.v10i2.42136
24. Elumalai K, Velmurugan S. Applied surface science green synthesis, characterization and antimicrobial activities of zink oxide nanoparticles from the leaf extract of *Azadirachta indica* (L.). *Applied Surface Science*. 2015;345:329–336. doi:10.1016/j.apsusc.2015.03.176
25. Zhang J, Sun LD, Yin JL, Su HL, et al. Control of ZnO morphology via a simple solution route. *Chemistry of Materials*, 2002;14(10):4172–4177. doi:10.1021/cm020077h
26. Saridewi N, Fidaus DA, Aziz I, Kamila BN, Dasumiati D. Biosynthesis of ZnO Nanoparticles Using Pumpkin Peel Extract (*Cucurbita moschata*) and its Applications as Semiconductor in Dye Sensitized Solar Cell (DSSC). *Jurnal Kimia Valensi*, 2021;7(2), 100–107. doi:10.15408/jkv.v7i2.21046
26. Gong J, Sumathy K, Qiao Q, Zhou Z. Review on dye-sensitized solar cells (DSSCs): Advanced techniques and research trends. *Renewable and Sustainable Energy Reviews*, 2017;68(P1):234–246. doi:10.1016/j.rser.2016.09.097

27. Dewi AK, Aryanto D, Nurbaiti U. Pengaruh Perlakuan Panas Terhadap Sifat Optik Lapisan Tipis ZnO Di Atas ITO. *Jurnal Fisika*, 2020;10(1):30–36. doi:10.15294/jf.v10i1.24580
28. Daniyati R, Zharvan V, Pramono YH. Penentuan Energi Celah Pita Optik Film TiO₂ Menggunakan Metode Tauc Plot. *Seminar Sains Dan Teknologi*, 2015;1(August):1–5.
29. Effendy. *Logam, Aloi, Semikonduktor dan Superkonduktor*. Malang: Bayumdhia Publishing; 2010.
30. Dahlan D, Leng TS, Aziz H. Dye Sensitized Solar Cells (DSSC) dengan Sensitiser Dye Alami Daun Pandan, Akar Kunyit dan Biji Beras Merah (Black Rice). *Jurnal Ilmu Fisika / Universitas Andalas*, 2016;8(1):1–8. doi:10.25077/jif.8.1.1-8.2016
31. Blok L, Bruyn PLD. The ionic double layer at the ZnO solution interface: I. The experimental point of zero charge. *Journal of Colloid and Interface Science*, 1970;32(3):518–526. doi:10.1016/j.envadv.2023.100381
32. Kosmulski M. The significance of the difference in the point of zero charge between rutile and anatase. *Advances in Colloid and Interface Science*, 2002;99(3):255–264. doi:10.1016/S0001-8686(02)00080-5
33. Janitabar-Darzi S, Mahjoub AR. Investigation of phase transformations and photocatalytic properties of sol-gel prepared nanostructured ZnO/TiO₂ composite. *Journal of Alloys and Compounds*, 2009;486(1-2):805–808. doi:10.1016/j.jallcom.2009.07.071
34. Wang M., Huang C, Cao Y, Yu Q, Deng Z, Liu Y, et al. Dye-sensitized solar cells based on nanoparticle-decorated ZnO/TiO₂ core/shell nanorod arrays. *Journal of Physics D: Applied Physics*, 2009;42(15):155–104. doi:10.1088/0022-3727/42/15/155104